Supporting Information: Direct Observation of Transient Surface Species during Ge Nanowire Growth and their Influence on Growth Stability

Authors: Saujan V. Sivaram, Naechul Shin, Li-Wei Chou, Michael A. Filler*

Affiliation: School of Chemical & Biomolecular Engineering, Georgia Institute of Technology, Atlanta, GA 30332, USA.

Kinetic Model:

We utilize a heterogeneous Ge_2H_6 decomposition mechanism that begins with the dual-site chemisorption reported by Chabal *et al.*:[43]

$$Ge_2H_6 + 2V \xrightarrow{k_1} (Ge_2H_5)_{ads} + H_{ads} \quad \text{(R1)}$$

$$(Ge_2H_5)_{ads} + V \xrightarrow{k_2} (Ge_2H_4)_{ads} + H_{ads} \quad \text{(R2)}$$

$$(Ge_2H_4)_{ads} + V \xrightarrow{k_3} 2(GeH_2)_{ads} \quad \text{(R3)}$$

$$2\left[(GeH_2)_{ads} + V \xrightarrow{k_4} 2H_{ads}\right] \quad \text{(R4)}$$

$$3\left[H_{ads} + H_{ads} \xrightarrow{k_5} H_2 + 2V\right] \quad \text{(R5)}$$

$$Ge_2H_6 \xrightarrow{k_{overall}} 2Ge + 3H_2 \quad \text{(R6)}$$

Here, 'V' refers to a vacant surface site. The surface site balance for this situation is:

$$1 = \theta_V + \theta_H + \theta_{GeH_2} + \theta_{Ge_2H_4} + \theta_{Ge_2H_5} \quad \text{(S1)}$$

where θ_j (j = V, H, GeH_2, Ge_2H_4, or Ge_2H_5) refers to the surface coverage of each species (i.e., surface sites occupied by species j divided by total number of surface sites). The coverage of vacant surface sites is θ_V. Since only monohydrides are observed in our spectra, as expected for the conditions examined here,[24,43] we know that k_2, k_3, $k_4 >> k_5$. The surface hydrogen atom coverage, θ_H, at steady-state is therefore determined by a competition between Ge_2H_6 adsorption (R1) and H_2 desorption (R5):

$$\frac{d\theta_H}{dt} = 0 = k_1\theta_V^2 p_{Ge_2H_6} - 2k_5\theta_H \quad \text{(S2)}$$

where k_1 and k_5 are the rate constants for R1 and R5, respectively, and $p_{Ge_2H_6}$ is the partial pressure of Ge_2H_6. Temperature-programmed desorption experiments indicate that desorption is first-order with respect to θ_H on Ge(100) surfaces.[22] The site balance simplifies to:

$$1 = \theta_V + \theta_H \tag{S3}$$

Solving for θ_V in Equation S3 and substituting in Equation S2, we obtain the following expression:

$$\frac{d\theta_H}{dt} = 0 = k_1(1-\theta_H)^2 p_{Ge_2H_6} - 2k_5\theta_H \tag{S4}$$

Rearranging and assuming k_1 and k_5 exhibit an Arrhenius dependence, we obtain:

$$\frac{(1-\theta_H)^2}{\theta_H} = \frac{2k_5}{k_1 p_{Ge_2H_6}} = \frac{2k_{5,o}}{k_{1,o} p_{Ge_2H_6}} e^{\frac{E_1 - E_5}{RT}} = \frac{\beta}{p_{Ge_2H_6}} e^{\frac{E_{net}}{RT}} \tag{S5}$$

where $k_{1,o}$, E_1 and $k_{5,o}$, E_5 are the pre-exponential factors and activation energies for the rate constants k_1 and k_5, respectively. Here, $\beta = {2k_{5,o}}/{k_{1,o}}$ and $E_{net} = E_1 - E_5$. We fit our experimental values for θ_H to this kinetic model by linearizing Equation S5 to yield:

$$\ln\left(\frac{(1-\theta_H)^2}{\theta_H}\right) = \ln\left(\frac{\beta}{P_{Ge_2H_6}}\right) + \frac{E_{net}}{RT} \tag{S6}$$

and plotting the left hand side of Equation S6 with respect to T^{-1}. Since k_1 and k_5 differ by crystal facet,[23,27] we find approximate values for E_{net} and β by fitting our θ_H values, even at different Ge_2H_6 partial pressures, simultaneously. As seen in Figure 7, the functional form is consistent with our experimental data.

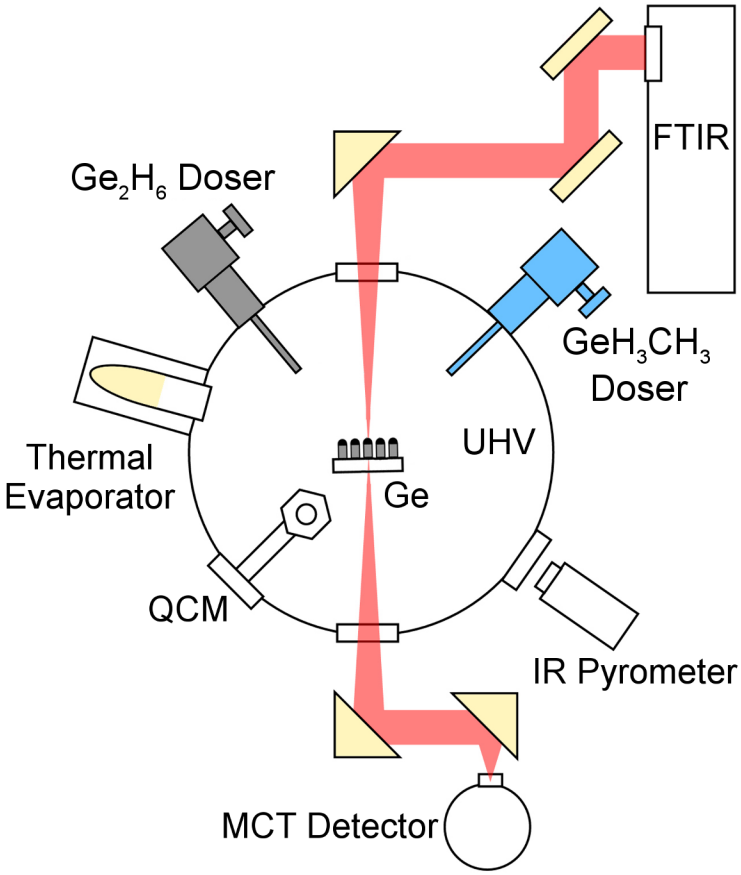

Figure S1. Experimental setup. Schematic of ultrahigh vacuum chamber (UHV) coupled with *in situ* transmission infrared spectroscopy. The infrared beam path is show in red. As seen in the schematic, the substrate is oriented perpendicular to the beam path for the nanowire *operando* and *saturation* measurements. During Au deposition the substrate is oriented perpendicular to the thermal evaporator. Film thickness is measured with a quartz crystal microbalance (QCM). Temperature is measured with an infrared (IR) pryometer focused on the backside on the Ge substrate. Ge_2H_6 is introduced through the leak valve and doser combination shown in gray, while GeH_3CH_3 is added through that shown in blue.

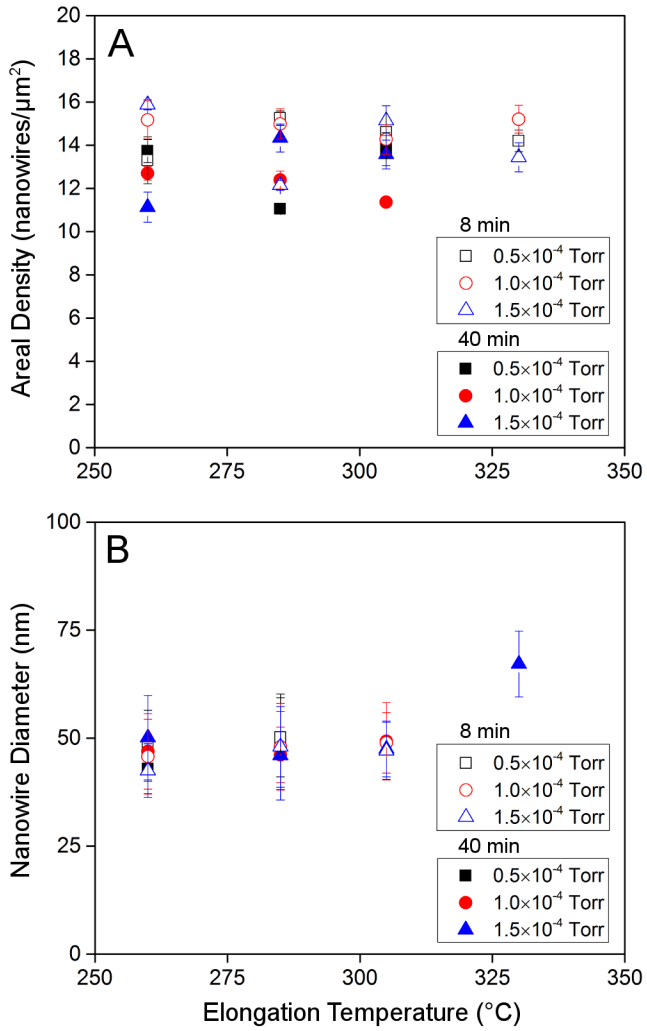

Figure S2. Nanowire statistics. Average (**A**) array areal densities (ρ) and (**B**) nanowire diameters as a function of T_{sub} and $p_{Ge_2H_6}$. Areal densities calculated from plan view SEM images (4.57 μm × 3.26 μm) taken at three different locations within ~10 μm from the substrate center. Diameter of 50 nanowires per growth condition, measured at the liquid-solid interface. Due to limited vertical yield, only 25 nanowires are sampled for T_{sub} = 330 °C and $p_{Ge_2H_6} = 1 \times 10^{-4}$ Torr. Vertical nanowire growth is not obtained for T_{sub} = 330 °C and $p_{Ge_2H_6} = 0.5 - 1 \times 10^{-4}$ Torr (see Figure 2).

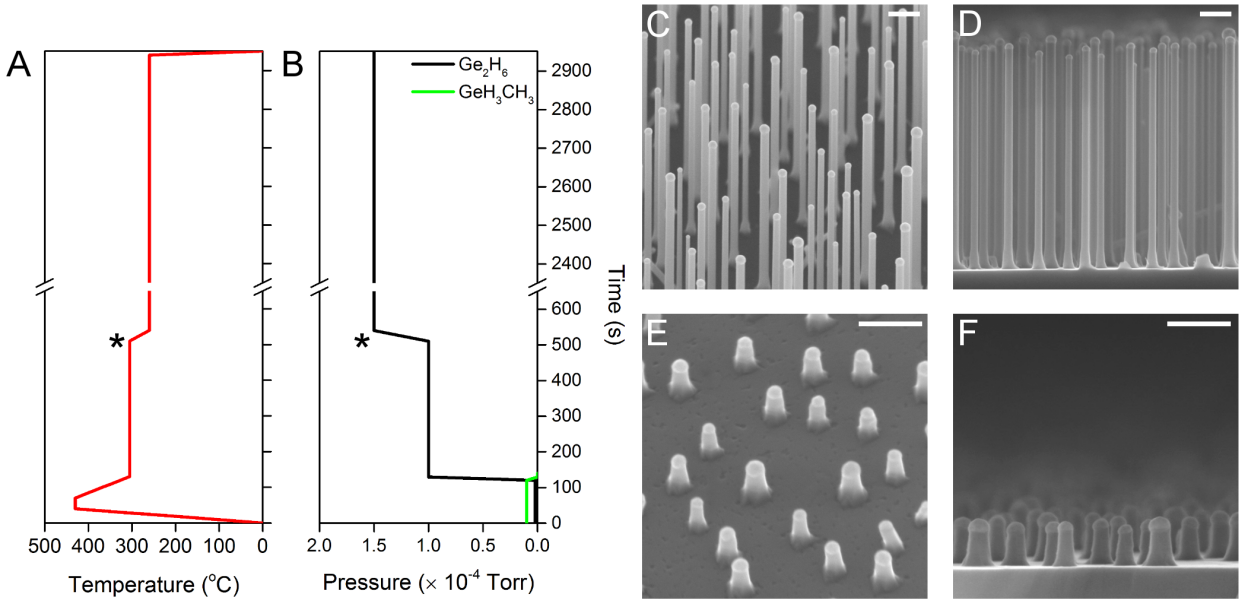

Figure S3. Nanowire synthesis protocol. Schematic plots of (**A**) substrate temperature (T_{sub}) and (**B**) precursor partial pressures ($p_{Ge_2H_6}$ and $p_{GeH_3CH_3}$) versus time for a typical nanowire synthesis. The procedure consists of an "incubation" step, which is the same for all nanowire growths, and subsequent "elongation" at a T_{sub} and $p_{Ge_2H_6}$ of interest. The transition between incubation and elongation is denoted with '*'. Representative (**C**) 45° and (**D**) side-view SEM images of a nanowire array elongated for 40 minutes at T_{sub} = 260 °C and $p_{Ge_2H_6}$ = 1.5 × 10^{-4} Torr. Terminating growth immediately after incubation yields ~100 nm long nanowires as shown in the (**E**) 45° and (**F**) side-view SEM images. Scale bars, 200 nm.

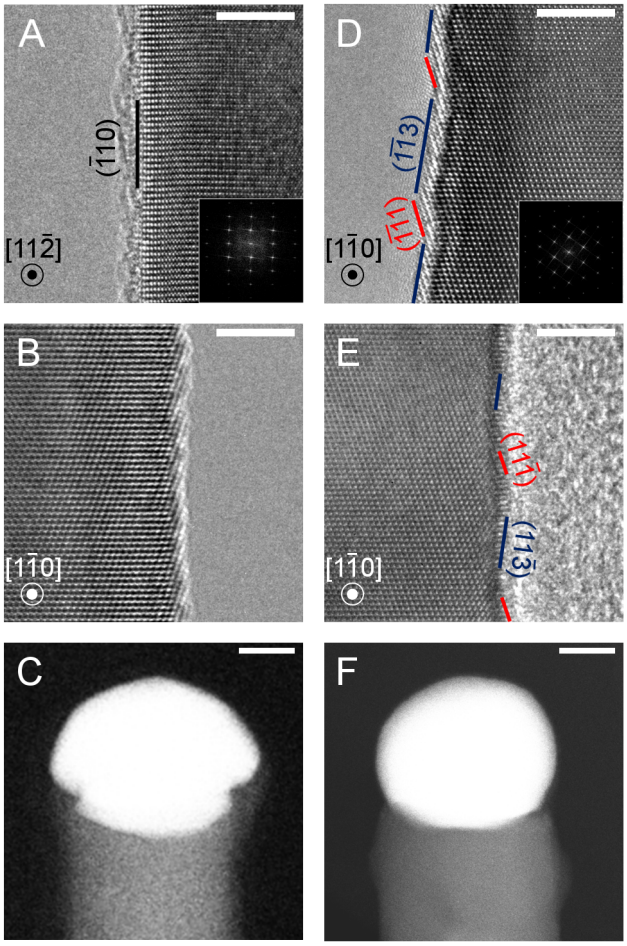

Figure S4. TEM analysis of tapered and untapered nanowires. Bright field high resolution TEM image of a representative Ge nanowire grown at T_{sub} = 260 °C and $p_{Ge_2H_6}$ = 1 × 10^{-4} Torr along the (**A**) $[11\bar{2}]$ and (**B**) $[1\,\bar{1}0]$ zone axes. Scale bars, 5 nm. (**C**) Dark field STEM image of the nanowire imaged in (A,B). Scale bar, 10 nm. Bright field high resolution TEM image of a representative Ge nanowire grown at T_{sub} = 305 °C and $p_{Ge_2H_6}$ = 1 × 10^{-4} Torr along the (**D**) $[11\bar{2}]$ and (**E**) $[1\,\bar{1}0]$ zone axes. Scale bars, 5 nm. (**F**) Dark field STEM image of the nanowire imaged in (D,E). Scale bar, 10 nm.

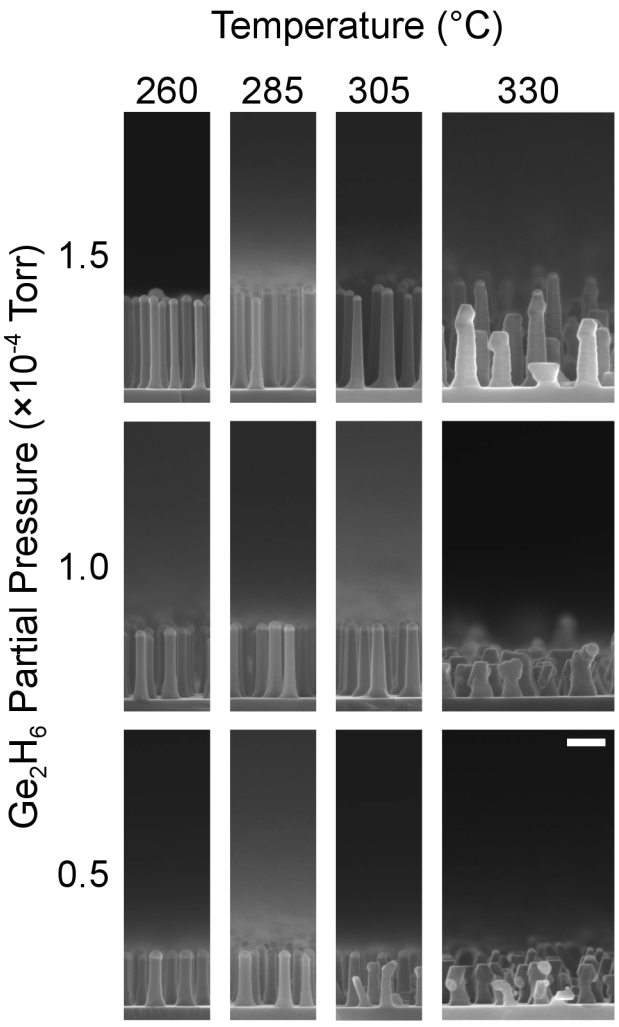

Figure S5. Nanowire morphology after elongation for 8 minutes. Representative side-view SEM images showing Ge nanowire morphology as a function of T_{sub} and $p_{Ge_2H_6}$ after elongation for 8 minutes. Scale bar, 200 nm.

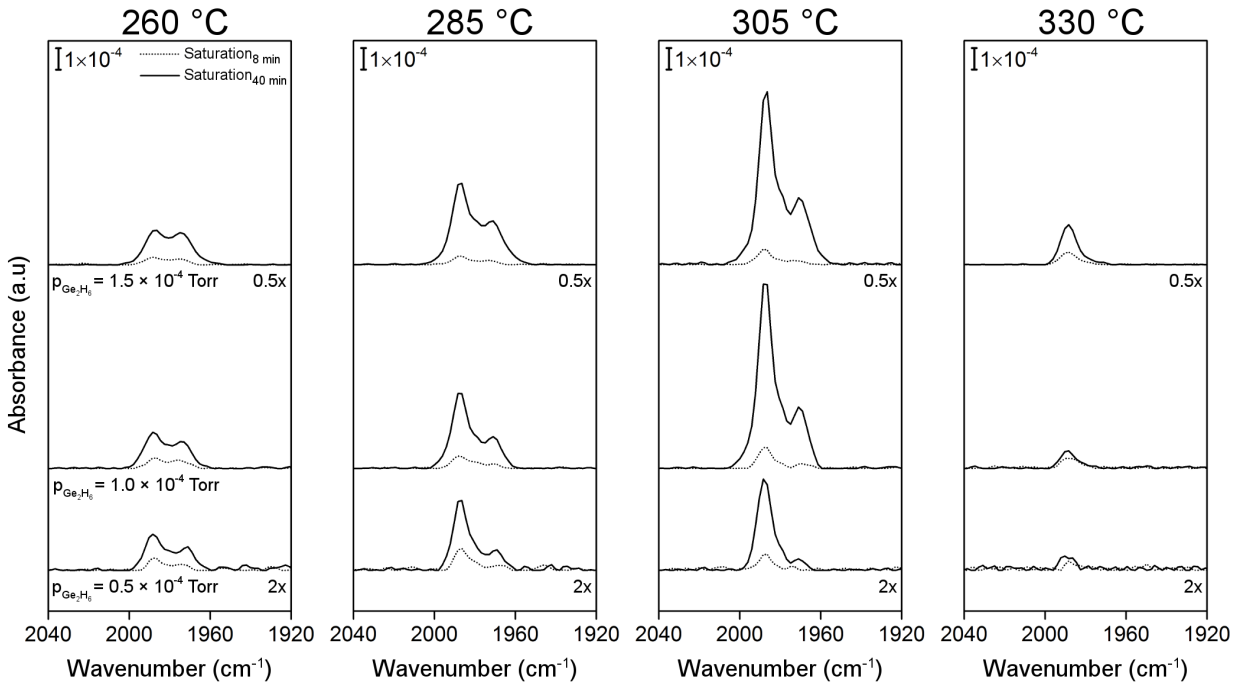

Figure S6. Comparison of post-growth saturation spectra. $A_{saturation_{40\min}}(\tilde{\nu})$ (solid) and $A_{saturation_{8\min}}(\tilde{\nu})$ (dotted) infrared absorption spectra recorded after 40 and 8 minute nanowire elongations, respectively, at the indicated T_{sub} and $p_{Ge_2H_6}$. Spectra for $p_{Ge_2H_6}$ = 0.5 and 1.5 × 10^{-4} Torr are scaled by a factor of 2 and 0.5, respectively, for ease of comparison. Background spectra are of the Au-covered Ge(111) substrate maintained at room temperature in vacuum immediately prior to nanowire growth. All spectra are recorded with the substrate oriented perpendicular to the beam path (see Figure 1A).

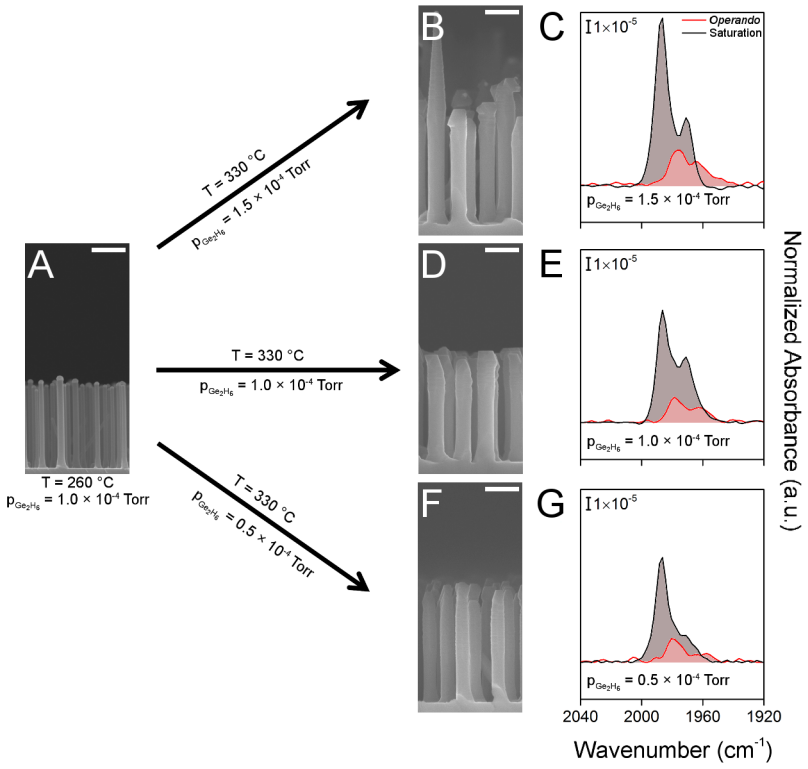

Figure S7. High surface area experiments. (**A**) Representative side-view SEM image of initial nanowire elongated for 40 minutes at T_{sub} = 260 °C and $p_{Ge_2H_6}$ = 1 × 10^{-4} Torr. (**B, D, F**) Representative side-view SEM images of nanowire arrays first grown as in (A) and then elongated for an additional 32 minutes at T_{sub} = 330 °C and the indicated Ge_2H_6 partial pressure. (**C, E, G**) Comparison of $A^{norm}_{operando}(\tilde{\nu})$ (red) and $A^{norm}_{saturation}(\tilde{\nu})$ (gray) for each condition shown in (B, D, F). All spectra are recorded with the substrate oriented perpendicular to the beam path (see Figure 1A).